KJ Lin & BG Thomas, China Steel Technical Report, No. 16, 2002, pp. 9-14.

Thermal Stress Analysis of Bulging with Roll Misalignment for Various Slab Cooling Intensities

KUAN-JU LIN [*] and BRIAN G. THOMAS[**]

Temperature, displacement, strain and stress fields in the solidifying strand of continuous steel slab casters were numerically investigated to understand bulging phenomena between support rolls. The thermal model accounted for heat transfer variations at the strand surface between rolls in the spray zones, including roll contact, direct spray impingement, convection, and radiation. Shell temperatures were calculated for different spray zone cooling designs and were validated with experimental measurements from thermocouples embedded in the solidifying steel shell. The results were further investigated with an elastic-plastic thermal-stress model. Roll misalignment was found to be a dominant factor in determining shell bulging. Moreover, the maximum bulging strain across the solidification front was found to correlate to about 2.4 times the ratio of maximum bulging displacement to roll pitch.

1. INTRODUCTION

The production of heavy plate with superior quality, based on performance in Charpy and ultra-sonic tests, is highly dependent on diminishing the centerline segregation and porosity in the strand during the continuous casting process. Since bulging arising from ferrostatic pressure on the solidifying shell between the support rolls is a major contributor to these quality problems(1), many investigations of strand bulging phenomena have been conducted, using modeling or inter-roll bulging measurements(15). These previous studies have established that the most important factors aggravating bulging are excessive roll pitch, hot surface temperature, shell fragility and excessive ferrostatic pressure. Moreover, increasing the casting speed has been found to be indirectly detrimental, because it causes a

hotter, thinner and thus weaker shell. Consequently, technologies to counter bulging problems, such as split rolls with shorter pitch[1-5], uniform and intensified secondary spray cooling[1-7] and controlled roll-gap taper including soft reduction during final solidification[8], have been developed to improve slab quality. Despite implementing these measures[9] to improve centerline segregation at the #1 slab continuous caster (#1SCC) in China Steel, centerline defects in heavy plate were still occasionally encountered during ultrasonic testing. Moreover, the intense cooling induced transverse cracks on the surface of Nb-containing slabs. In order to clarify the role of thermal effects and roll misalignment on shell bulging, this paper examines the temperature, stress, and strain fields in the steel strand, using computational models which are first validated with plant measurements.

2. MODEL DESCRIPTION

In this work, heat transfer in the solidifying steel strand was computed using the finite-difference code, CON1D,[18] and the resulting temperatures were input to a two-dimensional model of stress / strain fields in the shell, solved with the FEM code, ABAQUS. The model formulation and domain, casting conditions, and mechanical properties of steel at high temperature, are defined below.

2.1 Shell temperature and thickness calculation

The 1-D transient heat transfer model called CON1D, developed by the Continuous Casting Consortium at the University of Illinois at Urbana-Champaign, was adopted to calculate the variations of slab temperature in the continuous casting process. Previously measured temperatures[9] at #1SCC (air-mist cooling) and #3SCC (water cooling) were compared with the CON1D results to validate the model. The experiments were conducted by inserting thermocouples into the liquid pool in the mold. Temperatures in the strand where they solidified were continuously recorded during withdrawal[10].

2.2 Bulging, strain and stress calculation

The domain for the two-dimensional stress/strain analysis consists of a short length of shell suspended over two roll pitches by three support rolls, as shown in Fig.1. The domain thickness was taken from the predicted shell thickness from the CON1D results, assuming a solid fraction in the mushy zone of 70%, which corresponds to the zero strength

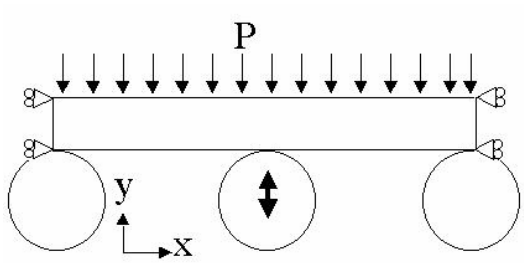

Fig.1. Conditions of the stress analytic domain

temperature.[11] The temperatures imposed at each node in the finite element mesh were extracted from the CON1D results. The shell is presumed static relative to the rolls regardless of any actual movement during casting and strand curvature was neglected. Contact between the hot shell and the rolls was modeled using contact elements, assuming the rolls to act as rigid bodies. Axial displacement (x-direction) of the two ends of the shell was fixed.

The magnitude of the ferrostatic pressure loading upon the rolls is proportional to the height of the free liquid steel surface, as expressed in Eq.1. The central roll was shifted out of vertical alignment (y direction) by displacing it 0.5, 2 or 5 mm from the initial flat shell surface, in order to simulate situations of roll misalignment. The bulging of the shell was quantified by the maximum computed displacement in the y-direction.

$$P = \rho g h \qquad \ldots (1)$$

2.3 Mechanical properties of steel at high temperature

Steel is subjected to simultaneous elastic and inelastic deformation due to plasticity and creep upon application of load in the temperature range of 900℃ to 1500℃ during the continuous casting process. This complex mechanical behavior was approximated by the elastic-plastic kinematic strain-hardening model in ABAQUS[12,13]. The elastic modulus was taken to be the function of temperature given in Eq. 2, as proposed by Kozlowski[14],

$$E = 968 - 2.33\times T + 1.90\times 10^{-3}\times T^2 - 5.18\times 10^{-7}\times T^3 \quad \ldots(2)$$

The temperature-dependent yield stress of steel was based on relations extracted from tensile test measurements at strain rates approximating those in continuous casting [15] and is given in Table 1.

Table 1. Kinematic strain-hardening yield stress (MPa) of steel at high temperature

Temperature , ℃	600	700	800	950	1100	1200	1400	1500
0% strain	208	130	64	20	12.7	10	3	0.5
5% strain	240	145	75	50	27.7	17.5	13	1.0

3. RESULTS AND DISCUSSIONS

3.1 Validation of heat transfer model

Several phenomena control heat extraction from the strand surface in the secondary cooling zones, including spray water cooling in the region of direct impingement, roll contact, radiation, and convection due to both natural air flow and the down-flow of residual water. The boundary conditions which characterize these four phenomena are specified in the CON1D model in overlapping regions, as shown in Fig.2.

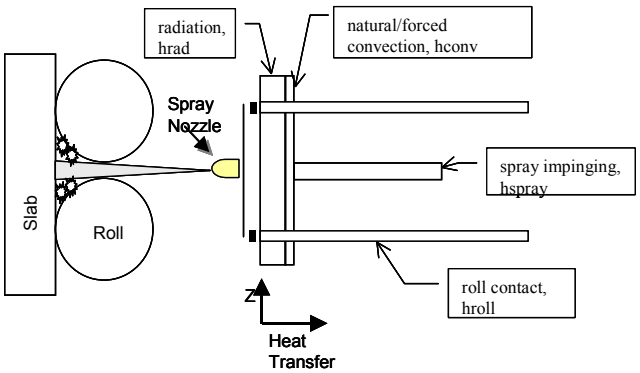

Fig. 2. Boundary conditions in a spray zone region in CON1D model

Eqs.3, 4 and 5 define the heat transfer coefficients due to spray cooling, radiation, and convection respectively.

$$h_{spray} = 1.57 \cdot Q_w^{\,0.55} \cdot \left(1 - 0.0075 \cdot T_{amb}\right) \cdot {}^{1}\!/_{\alpha} \qquad \ldots\ldots \quad (3)$$

$$h_{rad} = \sigma \cdot \varepsilon_{steeel} \cdot \left(T_s + T_{amb}\right) \cdot \left(T_s^{\,2} + T_{amb}^{\,2}\right) \qquad \ldots. \quad (4)$$

$$h_{conv} = Max(8.7,\ m \cdot Q_W) \qquad \ldots. \quad (5)$$

The spray cooling of Eq.3, based on in-plant actual temperature measurement, was originally proposed by M. Shimada et al.[16] and modified by T. Nozaki et al.[17] Radiation, Eq. 4, applies in all zones, except beneath the rolls.

The convection of Eq.5 has at least the value of 8.7 W/m^2.℃ for natural convection, assuming that spray water is negligible outside of the impingement zone. For spray mist cooling however, the coefficient is increased to account for the large volume of mist, which induces heat extraction even outside the region of direct impingement.

The temperature increase of the cooling water running through the support rolls of #1SCC was recorded to quantify the heat extraction from the strand by roll contact. Figure 3 shows that the water temperature rose rapidly in the first 30 minutes after the start of casting, as the first slab was being pulled through the caster. The temperature increased gently before

reaching steady state for most of the casting period. As the casting sequence was finished, the roll water temperature dropped steadily until the next casting sequence began. The total heat removed by the rolls can be estimated from the water temperature rise and flow rate. The heat removed from the slab surface in each roll contact was deduced to be 21.1 KW/m, by dividing the total heat removed by the number of the rolls and the slab width.

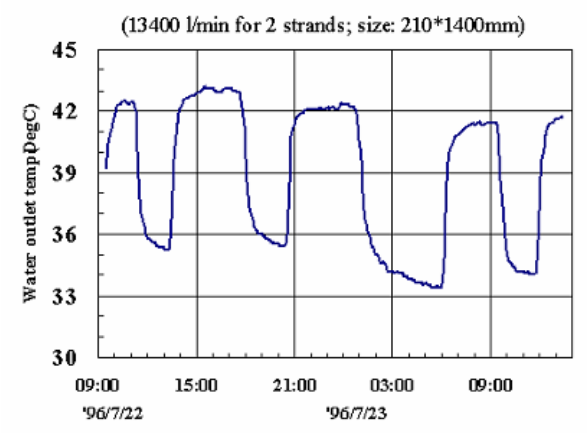

Fig. 3. Temperature of machine water at #1SCC

Figure 4 compares the measured and calculated temperatures in the case of water spray cooling at #3SCC, assuming the same heat extraction at each roll contact. The calculated temperatures at three points, 10 ㎜, 12.5 ㎜ and 100 ㎜ under the slab surface, were found to match closely to the experimental temperatures recorded in the secondary cooling zone.

Air-mist cooling, in contrast to water-spray cooling, is considered to have better cooling uniformity and efficiency, so is now used in many modern casters. Simply increasing the heat transfer coefficient in the impingement region for the air-mist nozzles did not produce a good match with the experiments, because it led to exaggerated fluctuation of surface

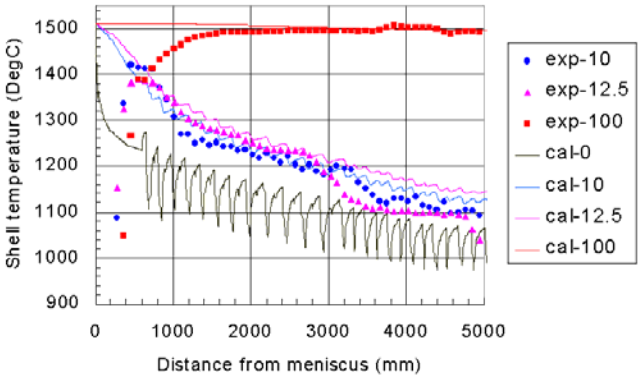

Fig.4. Comparison of experimental and calculated temperatures for water spray cooling

temperature. Thus, increased forced convection was inferred to be induced by the large volume of mist ejected throughout the compact chamber between each pair of rolls.

Incorporating forced convection with a coefficient (m) of 12.4 in Eq.4, produced good agreement between the measured and calculated temperatures for air-mist cooling, as shown in Fig.5. The various heat transfer coefficients on the slab surface are compared together in Fig.6. The convection coefficient for spray cooling was in the range of 200-700 W/m^2. ℃, depending on the water density. For roll contact, the coefficient exceeded 5000 W/m^2. ℃, owing to the relatively narrow contact area. For the air-mist cooling system, convection was as important as radiation in cooling the overall surface area.

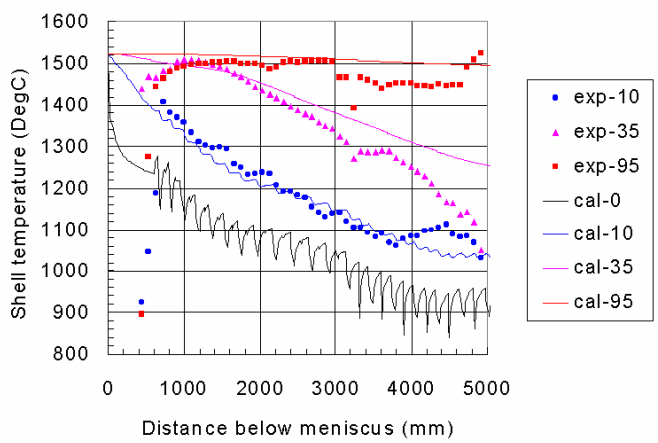

Fig. 5. Comparison of experimental and calculated temperatures for air-mist cooling

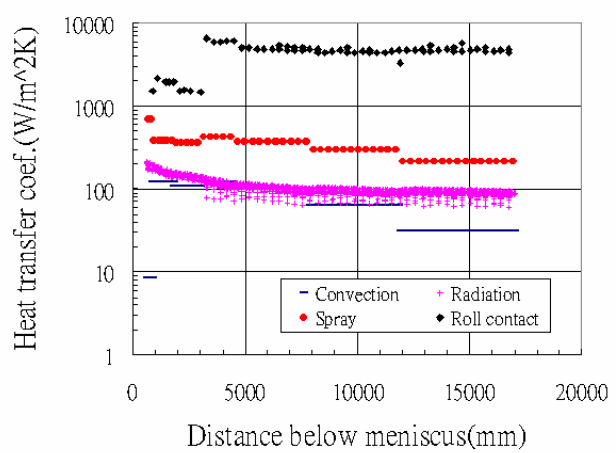

Fig. 6. Heat transfer coefficients on the surface of slab for air-mist cooling

3.2 Temperature variations of the solidifying shell with different cooling intensity

Three different cooling patterns (represented by soft, medium and strong cooling with specific water flows of 0.39, 0.6 and 1.2 l/kg.steel, respectively) were adopted to calculate strand thermal histories in the #1SCC continuous caster. Temperature profiles along the slab surface and center are compared in Fig.7. The surface temperatures repeatedly dropped and rebounded rapidly in the cooling zone, each time the strand passed beneath either a roll or a water-impingement region. It was found that the stronger the water density, the lower the surface temperature. Moreover, the crater end (metallurgical length) shorted by 0.8m for medium cooling and 1.5m for strong cooling, relative to that of soft cooling. Five locations in the strand were selected for bulging analysis, as shown in Table 2.

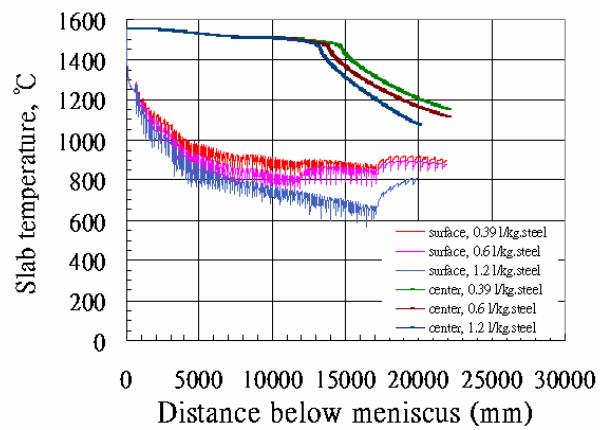

Fig. 7. Temperature Profiles of Slab with Various Cooling Pattern

Table 2. Conditions of shell in the strand for bulging analysis

Location below meniscus, m	Support rolls	Roll pitch, mm	Shell thickness, mm			pressure, MPa
			0.39 l/kg	0.6 l/kg	1.2 l/kg	
3.02-3.61	No.12-14	295	47.3-52.8	48.3-56	49.3-58	0.21-0.24
4.49-5.17	No.17-19	341	55.7-66.3	62.9-71.6	64.2-74.7	0.3-0.34
8.24-8.9	No.28-30	331	93.7-99.4	98.7-102.6	101.3-104.5	0.51-0.54
11.7-12.4	No.38-40	350	112.1-121.2	122.1-128	127.1-131.9	0.65-0.67
13.27-13.97	No.43-45	350	129.9-134.5	135	135	0.69-0.7

3.3 Bulging analysis of the solid shell

Bulging displacement of the shell with soft cooling between the 12th and the 14th rolls was analyzed with roll misalignment in the range of 0-5 ㎜. It was found that bulging was less than 0.1 ㎜ without roll misalignment, as shown in Fig.8. The shell with soft cooling generally bulged exactly as much as the roll was misaligned. With stronger cooling, however, the resulting thicker shell and lower temperatures sometimes lowered shell bulging to less than the roll misalignment, as also illustrated in Fig.8. When the middle support roll was absent, the maximum bulging deformation of the shell was 2.59 ㎜ for medium cooling and 1.47 ㎜ for strong cooling. This decrease is because the stronger cooling alone strengthened the solid shell to withstand the ferrostatic pressure. However, this limited improvement in bulging from increased water intensity was much less important than roll misalignment, which dominated the extent of bulge displacement.

As the shell grows thicker during strand withdrawal, the ferrostatic pressure increases as well. The maximum bulging displacements at different positions along the strand are compared in Fig.9. The pitch design for the support rolls of the strand in #1SCC are observed to well-satisfy the requirements to ensure slab quality, as slab bulging is consistently less than 0.1 ㎜. Thus, the maintenance of the roll position as well as the prevention of roll bending and wear is demonstrated to be important. Roll misalignment,

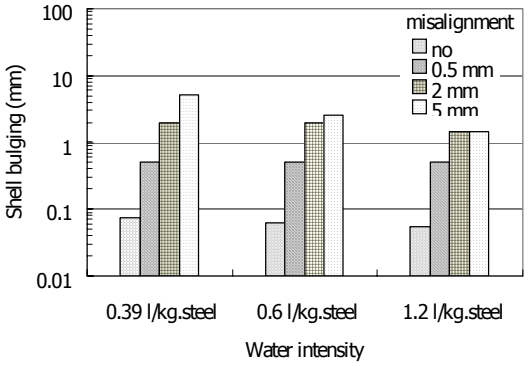

Fig. 8. Effect of water intensity and roll misalignment on the shell bulging

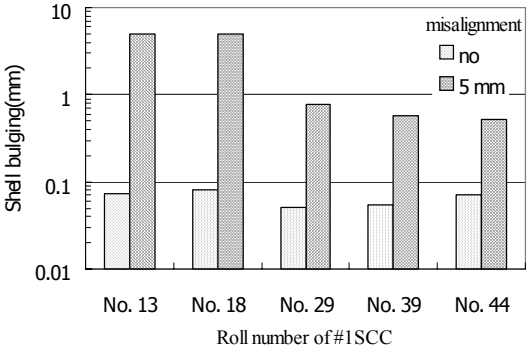

Fig. 9. Comparison of shell bulging at the different roll position

particularly in the region of final solidification, might deteriorate segregation quality.

3.4 Maximum strain on the solidification front

The results from the bulging analysis were regressed to produce a relationship to predict the total strain across the solidification front. Fig.10 shows that the detrimental bulging strain is predicted well with a simple linear equation. The maximum strain on the solidification front equals about 2.4 times the ratio of maximum bulging displacement to roll pitch. This simple equation can be further applied to deduce the roll misalignment allowable during maintenance to keep the solidifying shell away from cracking.

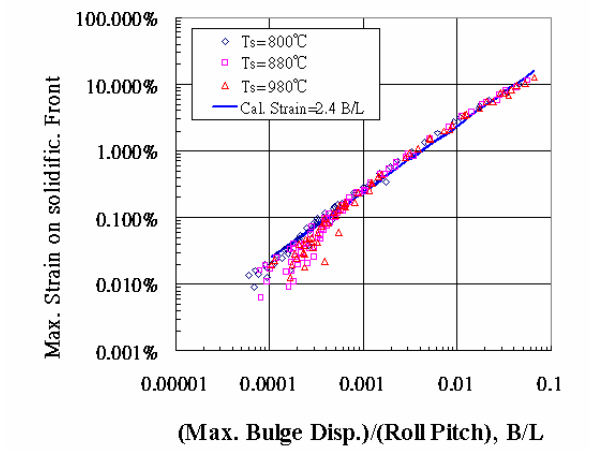

Fig.10. Correlation between max. bulge displacement and strain on solidification front

4. CONCLUSIONS

Bulging phenomena in continuous casting were elucidated by computational investigation of the temperature and stress fields in the solidifying shell. The following findings were obtained:

1. The solidifying shell generally bulged exactly as much as the roll was misaligned. Increasing water intensity to strengthen the shell to better withstand the ferrostatic pressure was found to produce little improvement by itself, because roll misalignment dominated the bulge displacement.
2. The bulging strain could be reasonably predicted with a simple linear equation. The maximum strain on the solidification is about 2.4 times the ratio of maximum bulging displacement to roll pitch.

3. The various heat transfer coefficients on the slab surface were evaluated. Spray cooling coefficients were found to range between 200-700 W/m^2.℃, depending on the water density. The heat transfer by roll contact may exceed 5000 W/m^2.℃. The forced convection induced by the large volume of ejected mist plays a major role in enhancing the cooling efficiency of air-mist nozzles.

NOMENCLATURE

E : Young's modulus(Gpa)

T : steel temperature(Kelvin)
P : ferrostatic pressure(Mpa)
ρ : density of liquid steel(kg/m3)
g : gravity parameter(m/s2)

h : height of free liquid surface(m)

σ : Stefan Boltzman constant (5.67×10^{-8} W/m^{2}K^4)
ε_{steel} : steel emissivity
T_s , T_{amb} : steel surface temperature, ambient temperature (K)
m : coefficient for forced convection of air-mist nozzle
Qw : water flux (l/m^{2}sec)
α : coefficient proposed by Nozaki [17] for spray heat transfer

ACKNOWLEDGEMENTS

The authors wish to thank the graduate students, Ya Meng, Lan Yu and Chunsheng Li, in the Continuous Casting Consortium at the University of Illinois for their grateful assistance in coding the thermal and stress analysis models.

REFERENCES

1. T. Saeki, H. Imura, Y. Oonishi and H. Niimi: Transactions ISIJ, 1984, vol. 24, pp. 907-916

2. M. Yamada, S. Ogibayashi, M. Tezuka and T. Mukai: “Production of Hydrogen Induced Cracking Resistant Steel by CC Soft Reduction”; pp.77-85 in Steelmaking Conference Proceedings, vol. 71, Toronto, Apr. 17-20, 1988
3. M. Hashio, Y. Tozaki, T. Watanabe and J.I. Yoshiyama: "Slab Quality Improvement by Revamping No.1 Continuous Caster at Kashima Steel Works"; pp. 87-93 in Steelmaking Conference Proceedings, vol. 71, Toronto, Apr. 17-20, 1988
4. L.K. Chiang: "Application of Soft Reduction Technique for Improving Centerline Segregation in Continuously Cast Slab"; pp. 81-89 in Steelmaking Conference Proceedings, vol. 72, Chicago, Apr. 2-5, 1989
5. T. Kitagawa, M. Suzuki, T. Masaoka, S. Mizuoka, H. Kobayashi and Y. Tsuchida: NKK Tech. Report, 1988, No.121, pp.1-8
6. Y. Tsuchida, M. Nakada, I. Sugawara, S. Miyahara, K. Murakami and S. Tokushige: Transactions ISIJ, 1984, vol. 24, pp. 899-906
7. H. Kondo, R. Nishimachi, A. Tagane and K. Mori: NKK Technical Review, 1998, No. 79, pp. 1-7
8. M. Hattori, S. Nagata, A. Inaba, S. Ishitobi, T. Yamamoto, T. Okada and M. Zeze: “Development of Technology for Elimination of Segregation in Continuously Cast Slabs”; pp. 91-96 in Steelmaking Conference Proceedings, vol. 72, Chicago, Apr. 2-5, 1989
9. D. Sediako, K. J. Lin, S. Y. Lee, C. H. Huang, C. C. Lin and J. C. Lin: “Transverse Cracking Prevention and Segregation Reduction in Slab Continuous Casting”; pp. 351-357 in Steelmaking Conference Proceedings, vol. 80, Chicago, Apr. 13-16, 1997
10. Y. K. Chen, F. A. Feng, K. J. Lin and D. Sediako: “Improvement of Center Segregation for High Carbon Steel Bloom”; pp.505-512 in Steelmaking Conference Proceedings, vol. 79, Pittsburgh, Mar. 24-27, 1996
11. G. Shin, T. Kajitani, T. Suzuki and T. Umeda: Tetsu-to-Hagane, 1992, No. 4, pp. 587-593
12. M. Uehara, I.V. Samarasekera and J.K.Brimacmbe: Ironmaking and Steelmaking, 1986, vol. 13, No. 3, pp. 138-153
13. A. Grill and K. Schwerdtfeger: Ironmaking and Steelmaking, 1979, No. 3, pp. 131-135
14. P. Kozlowski, B.G. Thomas, J. Azzi and H. Wang: Metallurgical Transactions A, 1992, vol. 23A(March), pp125-134
15. L. Yu, “Bulging in Continuous Cast Steel Slabs”, M.S. Thesis, University of Illinois, 2000
16. M. Shimada and M. Mitsutsuka: Tetsu-to-Hagane, 1966, vol. 52, pp. 1643
17. T. Nozaki, J. Matsuno, K. Murata, H. Ooi and Kodama: Trans ISIJ, 1978, vol. 18, pp. 330-338
18. Y. Meng and B.G. Thomas, “Heat Transfer and Solidification Model of Continuous Slab Casting: CON1D”, submitted to Metallurgical and Materials Transactions, Aug., 2002.